

# Groundwater fluxes into a submerged sinkhole area, Central Italy, using radon and water chemistry

P. Tuccimei \*, R. Salvati, G. Capelli, M.C. Delitala, P. Primavera

*Dipartimento di Scienze Geologiche, Università "Roma Tre", Largo San Leonardo Murialdo 1, 00146 Roma, Italy*

Received 3 March 2004; accepted 30 April 2005

Editorial handling by R. Fuge

Available online 18 July 2005

## Abstract

The groundwater contribution into Green Lake and Black Lake (Vescovo Lakes Group), two cover collapse sinkholes in Pontina Plain (Central Italy), was estimated using water chemistry and a  $^{222}\text{Rn}$  budget. These data can constrain the interactions between sinkholes and deep seated fluid circulation, with a special focus on the possibility of the bedrock karst aquifer feeding the lake. The Rn budget accounted for all quantifiable surface and subsurface input and output fluxes including the flux across the sediment–water interface. The total value of groundwater discharge into Green Lake and Black Lake ( $\sim 540 \pm 160 \text{ L s}^{-1}$ ) obtained from the Rn budget is lower than, but comparable with historical data on the springs group discharge estimated in the same period of the year ( $800 \pm 90 \text{ L s}^{-1}$ ). Besides being an indirect test for the reliability of the Rn-budget “tool”, it confirms that both Green and Black Lake are effectively springs and not simply “water filled” sinkholes. New data on the water chemistry and the groundwater fluxes into the sinkhole area of Vescovo Lakes allows the assessment of the mechanism responsible for sinkhole formation in Pontina Plain and suggests the necessity of monitoring the changes of physical and chemical parameters of groundwater below the plain in order to mitigate the associated risk.

© 2005 Elsevier Ltd. All rights reserved.

## 1. Introduction

The development of catastrophic ground collapses in karst areas poses many problems for construction and other economic development and is nowadays viewed as a geohazard. Apart from overexploitation or pollution of karstic ground water, this is perhaps the most widespread problem encountered in karst terrains. The natural processes forming sinkholes can be enhanced by man-induced changes in the groundwater hydrologic regime. In order to draw up geohazard maps and specify the risk

intensity for each zone, it is necessary to understand the mechanisms and processes involved with sinkhole formation. This paper is focused on the role of deep seated fluids ascending along fault systems bordering a karst ridge (Lepini Mountains, Central Italy) and mixing with  $\text{Ca-HCO}_3$  type water from the karst aquifer. The tendency of these ground waters to dissolve  $\text{CaCO}_3$  is investigated and correlated with the development of collapse sinkholes affecting the sedimentary sequence covering the buried Mesozoic–Cenozoic limestone in an elongated down-thrown area (Pontina Plain) which borders the ridge.

The Pontina Plain (Fig. 1) has been affected by sinkhole activity at least since the end of the 19th century. Sinkhole occurrence is limited to a narrow strip between the western border of Lepini Mountains and the S.S.7

\* Corresponding author. Tel.: +39 06 5488 8092; fax: +39 06 5488 8201.

E-mail address: [tuccimei@uniroma3.it](mailto:tuccimei@uniroma3.it) (P. Tuccimei).

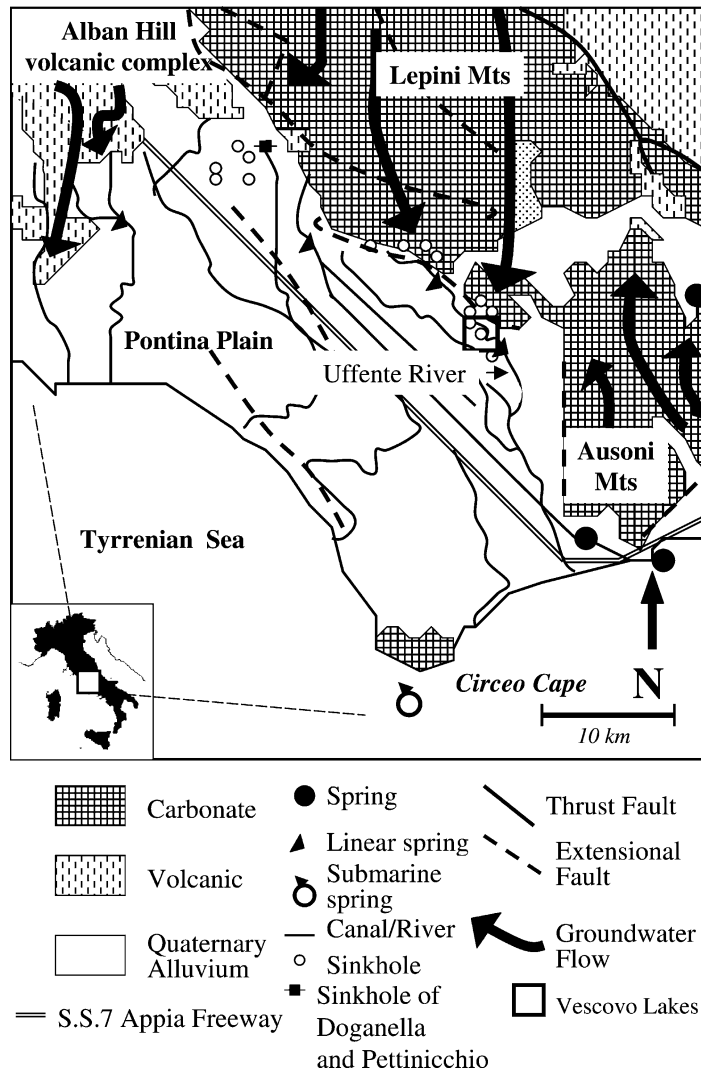


Fig. 1. Geological setting of Pontina Plain (Central Italy).

Appia freeway. Their density and distribution is less than in other areas of Central Italy (Salvati and Sasowsky, 2002), but they represent a potential hazard as shown by the two latest occurrences. The “sinkhole of Doganella” occurred in 1989 along a country road, breaking the pavement and barring the subsequent use of the road (Bono, 1995). The “Pettinicchio sinkhole” occurred in 1995 a few metres away from the S.S. Appia freeway and close to an electric power station.

Topographic maps from the 1920s show numerous circular depressions throughout the area. However, land reclamation for urban development has covered and filled most of those depressions, leaving only a few visible. Sinkhole distribution seems to be influenced by tectonic patterns, as they are oriented in directions very similar to the Lepini Mountains west border fault strikes.

During an evaluation of sinkholes in two regions of central Italy (San Vittorino Plain area and Pontina Plain), Capelli et al. (2000) and Salvati and Sasowsky (2002) recognized the development of cover collapse sinkholes. Sinkholes were found not in the recharge zone of the aquifer as they usually occur, but within the discharge zone, near the base of karst ridges, in areas with major groundwater circulation, thick overburden and proximity to deep-source gas or thermal upwelling. Salvati and Sasowsky (2002) hypothesised that recharge occurs on the limestone uplands, through both sinkhole and diffuse infiltration. Much of the water resurges in springs near the boundary between the Pontina Plain and the carbonate massif, joining a series of streams and canals that drain to the Tyrrhenian Sea. The authors considered that it is unlikely that sinkholes in this peculiar geological and hydrogeological setting can develop

from a simple ravelling process. The potential mechanism they invoked for removal of mass from the system and thus for sinkhole formation is the creation of voids at depth below the plain, either at the bedrock/sediment interface, or within the calcareous sediments within the overburden. This implies that water is aggressive to calcite in order to create the void. Such conditions can be brought up by either very short flowpaths (water never approaches saturation with respect to calcite) or by renewed undersaturated condition in long flow paths. The latter may be brought about by deep CO<sub>2</sub> gaseous sources ascending along bordering fault systems and interacting with the Ca–HCO<sub>3</sub> type water from a karst aquifer (Capelli et al., 2000; Salvati and Sasowsky, 2002). The hydration of deep CO<sub>2</sub> produces H<sub>2</sub>CO<sub>3</sub> which, in turn, dissociates to provide abundant H<sup>+</sup> and HCO<sub>3</sub><sup>-</sup>. The addition of H<sup>+</sup> related to this process enhances the CaCO<sub>3</sub> solubility.

In order to better assess the mechanism responsible for sinkhole formation in Pontina Plain and to verify the conceptual model formulated by Salvati and Sasowsky (2002), a <sup>222</sup>Rn budget, supplemented with physical and geochemical characterisation of sinkhole and spring waters, is applied to Green Lake and Black Lake, two sinkholes belonging to Vescovo Lakes Group (Fig. 1).

<sup>222</sup>Rn can be used as a natural tracer of groundwater flow into surface water because it has the following characteristics: (1) it is chemically conservative; (2) its concentrations in groundwater are much higher with respect to surface water.

The large difference in activity between groundwater and surface water allows <sup>222</sup>Rn to be used as a tracer of groundwater discharge into streams and rivers (Ellins et al., 1990; Smith, 2002; Cook et al., 2003), creeks (Lee and Hollyday, 1993), coastal plain estuary (Schwartz, 2003), coastal ocean (Cable et al., 1996; Lambert and Burnett, 2003) and surface reservoirs (Corbett et al., 1997). Snow and Spalding (1997) estimated short-term aquifer residence times from <sup>222</sup>Rn disequilibrium in artificially-recharged groundwater. Chanton et al. (2003) used <sup>222</sup>Rn to model the seepage rate variability in Florida Bay as a consequence of the Atlantic tidal height. By application of a Rn budget, Cable et al. (1996), Corbett et al. (1997, 2000) and Springer (2004) quantified the advective flux of groundwater into overlying surface water and from that estimated the velocity of advective fluids and the groundwater discharge.

The main advantage of using Rn, instead of other conservative elements, as a tracer of groundwater fluxes is that the Rn budget can be applied to calculate the groundwater discharge into lakes or other bodies of surface water, in place of a standard hydrological budget, or combined with it, whereas other conservative element budgets (e.g., chlorides) provide stock data that necessarily need to be supplemented with hydrologic balance calculations in order to give estimates of element inputs

and outputs (Moustafa et al., 1998; Michard et al., 2001) and from those infer the groundwater discharge.

## 2. Geological and hydrogeological setting

The Pontina Plain is the southernmost portion of an elongated downthrown area that developed between the first Apennine belt ridges and the shoreline starting in the Lower Pliocene. This depression is located between the Ausoni and Lepini Mountains (carbonate platform facies) to the East and the current Tyrrhenian margin (where calcareous-siliceous-marl deposits form the Mesozoic–Cenozoic buried bedrock) to the West (Fig. 1). The structural setting of the Pontina Plain is complicated by the existence of NE–SW trending secondary tectonic elements accompanying the general geological-structural evolution of this sector.

An interpretation of deep borehole and geophysical investigation data shows that the carbonate ridges extend below the Quaternary sediments with a tiered geometry, due to the presence of normal fault sets that cut the carbonate structures. Stratigraphic data show that above the Mesozoic–Cenozoic limestone deposits, the following sequence is found:

- Upper Pliocene clay passing to calcarenite in the sectors closer the Lepini ridge.
- Lower Pleistocene clay.
- Middle Pleistocene littoral deposits passing to saltier transitional deposits. These sediments contain large amounts of reworked pyroclastic deposits.
- Marine and transitional clays, sands and gravels deposited during the Upper Pleistocene. Northward of the Plain, volcanic activity of the Colli Albani complex was initiated.
- Large amounts of peat deposited in the continental fluvio-lacustrine basins during the Holocene.

The Pontina Plain sedimentary succession first developed from a marine depositional system to a transitional fluvial–coastal system, and then to a fluvial–continental depositional system (all of this within the Pliocene–Pleistocene). Therefore, the entire system is characterized by both vertical and lateral variability.

The hydrogeological setting, typical for Italian scenarios, is strongly constrained by the geological-structural setting. The following hydrogeological units can be identified:

- The Lepini karst ridge unit, characterised by a heterogeneous distribution of permeability, (inferred by the extreme variability of transmissivity values ranging from  $1 \times 10^{-1}$  to  $9 \times 10^{-5}$  m<sup>2</sup>/s), hydraulic gradients of 5–6 m/km, a constant regime of spring

discharges probably due to the lack of intersection between the karst network and the springs (Boni et al., 1980; Petitta, 1994) and Ca–HCO<sub>3</sub> type waters.

- An equivalent part of the same unit, downfaulted southwestward and covered by post-orogenic and quaternary deposits, in direct connection with the Lepini karst ridge unit (Boni et al., 1980).
- Quaternary alluvial and fluvio-coastal facies deposits that built up the Pontina Plain, hosting an unconfined aquifer and underlying semi-confined aquifers of limited extent, characterised by variable salinity and chemistry reflecting the heterogeneity of lithological types.

In addition to these groundwater circuits, a hydrothermal circuit exists in the buried karst bedrock of the Plain, with the main hydrogeological circulation along the fault network (Boni et al., 1980).

The river network in the plain is mainly fed by several springs located along the Lepini western border, and the total discharge amount can be estimated at 15 m<sup>3</sup>/s (Boni et al., 1980). Springs that drain the karst ridge are mainly discrete orifices, though some stream-bottom springs are found along the Uffente River where it flows close to the ridge border (Fig. 1).

Vescovo Lakes, located along the Lepini ridge border, is a group of sinkholes with spring-like features draining the Lepini karst aquifer (Fig. 1). The group is located at –1/–1.5 m above sea level (asl) and extends for about 200,000 m<sup>2</sup>. It consists of 4 main sinkholes (Green Lake, Black Lake, White Lake and Small Lake) with some minor springs. The average discharge of Vescovo Lakes is 890 L s<sup>–1</sup>, with maximum values of 1250 and minimum of 640 L s<sup>–1</sup> (Camponeschi and Nolasco, 1983). The lakes are surrounded by a low-lying wet land, covered at places by a floating mat of aquatic plants. This intricate vegetation makes the access to the central part of the area difficult. Green Lake and Black Lake (formed by the coalescence of two smaller lakes, hereafter called North Black Lake and South Black Lake) are located on the eastern side of the spring area and can be more easily reached.

### 3. Sampling and analyses

Sampling of Green Lake for water chemistry and Rn analyses was performed in June 2002, and during the following summer season (July 2003), sampling was extended to Black Lake. Water samples from Green Lake were collected in top-to-bottom profiles at 2 m intervals from 5 sampling stations (see Fig. 2(a)). The same procedure was adopted for Black Lake where 7 sampling locations were chosen (Fig. 2(b)). In June 2002 sampling included waters of springs (Sg13 and

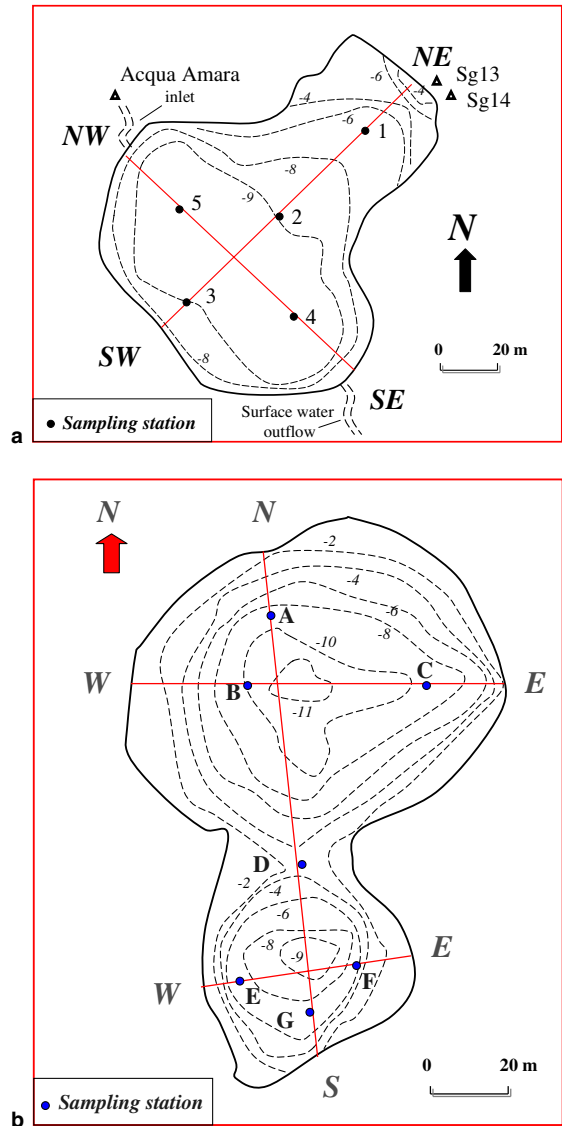


Fig. 2. Sampling stations at Green Lake ((a), with location of springs Sg13, Sg14, Acqua Amara spring – Camponeschi and Nolasco, 1983 –, Acqua Amara inlet and surface water outflow) and Black Lake (b). Dashed lines indicate isolines of water depth, m; solid lines stand for sampling transects.

Sg14) emerging at the NE edge of Green Lake along the Lepini Mounts border (Fig. 2(a)).

Temperature, pH, electrical conductivity (EC) and alkalinity were measured in the field using electric probes and, for alkalinity, by titration with 0.02 N HCl. The measurements of pH were accurate and reproducible to 0.1 pH units. The precision of the conductivity meter used for the analyses was about 1%.

The determination of Ca<sup>2+</sup>, Mg<sup>2+</sup>, Na<sup>+</sup>, K<sup>+</sup>, Cl<sup>–</sup>, F<sup>–</sup> and SO<sub>4</sub><sup>2–</sup> was performed in the laboratory on samples

filtered using 0.45  $\mu\text{m}$  Millipore. Calcium<sup>2+</sup> and Mg<sup>2+</sup> were measured using an EDTA titration method, Na<sup>+</sup> and K<sup>+</sup> by flame emission photometry, Cl<sup>-</sup> and F<sup>-</sup> by potentiometric methods with ion-selective electrodes, SO<sub>4</sub><sup>2-</sup> by a molecular absorption spectrometric method using the Merck Spectroquant Sulfate Test 1.14791 (Standard Methods for the Examination of Water and Wastewater, 1995). The precision of photometric, potentiometric and molecular absorption spectrometric measurements was always better than 0.5%. The accuracy of analyses was evaluated by calculating the anion–cation balance. The acceptable percentage difference is  $\pm 5\%$  for samples whose anionic sum ranges from 10.0 to 800 meq/L (Standard Methods for the Examination of Water and Wastewater, 1995). The calculated percentage difference of water samples from Green Lake and Black Lake is always within a difference of  $\pm 3\%$ . Another accuracy test for the analyses of water is the ratio of calculated total dissolved solids (TDS) to EC. The acceptable criteria for this ratio are from 0.55 to 0.7 (Standard Methods for the Examination of Water and Wastewater, 1995). The ratios of TDS to EC of analysed samples always fell within the range 0.56–0.66.

The Saturation Index with respect to calcite (SI) of water samples from Green Lake and Black Lake has been determined as the difference between measured pH and the pH of waters if they were in equilibrium with CaCO<sub>3</sub> at the existing Ca and HCO<sub>3</sub> ion concentrations. The adopted calculation estimates the ionic strength from the complete mineral analysis of water samples with a precision within the range of  $\pm 0.2$ .

Radon samples were collected in 250 or 40 mL evacuated bottles which were immediately sealed to prevent gas loss. Rn was extracted from water and counted using a continuous Rn Gas Monitor, model RAD7 produced by the DurrIDGE Company, 7 Railroad Avenue D, Bedford, MA 01730, equipped with a solid-state ion-implanted, planar, silicon alpha detector. Samples were run a second time (about 20 days later) for assay of <sup>226</sup>Ra by measuring <sup>222</sup>Rn ingrowth, assuming that Rn has completely gassed out at the first measurement. “Excess” Rn was determined as the difference between the “total” <sup>222</sup>Rn at the time of sampling and the supported <sup>222</sup>Rn, assumed to be equal to the <sup>226</sup>Ra activity. The value of unsupported Rn was decay-corrected back to the time of sampling to assess the in situ “excess” Rn concentrations. All Rn results are excess Rn values unless otherwise noted. The precisions of total Rn measurements ranged between 0.5% and 4% and those of Ra, and “excess” Rn were about 20–25%.

Radon was also measured in air just above the lake surface to estimate the gas exchange across the air–water interface that represents a potential loss of Rn from lake (see Section 5.2).

A bottom sediment grab sample was also collected in Green Lake by a diver along with lake water in order to

assess the potential diffusive flux of <sup>222</sup>Rn from sediments (see Section 4.5). This flux was obtained by equilibrating about 80 g wet sediment with 300 mL of lake water in a sealed container (Corbett et al., 1997) over a period of 30 days. After this time period, the equilibration activity of Rn supported by Ra in the sediment was established and the <sup>222</sup>Rn activity in the water phase was measured using the above mentioned continuous Rn Gas Monitor.

## 4. Theory

### 4.1. General radon model

Concentrations of <sup>222</sup>Rn in groundwater can be orders of magnitude greater than in overlying surface water mainly because of the release of <sup>222</sup>Rn atoms from mineral grains within the aqueous phase through the alpha-recoil effect (Wiegand, 2001). This large difference in activity allows <sup>222</sup>Rn to be used as a tracer of groundwater discharge into standing bodies of water. Here, the groundwater contribution into Green Lake and Black Lake (Vescovo Lakes Group) was estimated using a <sup>222</sup>Rn budget to assist in constraining hydrological and geochemical features of deep seated fluids ascending along the fault system bordering the Lepini Mounts karst ridge. The Rn budget is a balance of all quantifiable input and output fluxes of <sup>222</sup>Rn within a standing body of water. A simple box model may be used to describe all flux terms supporting water column inventories of <sup>222</sup>Rn:

- (1) flux of Rn across the sediment–water interface ( $J_{\text{benthic}}$ ) consisting of a diffusion component of Rn from bottom sediments into overlying lake water ( $J_{\text{diffusion}}$ ) and an advective component of Rn-rich groundwater through sediments ( $J_{\text{advective}}$ );
- (2) production of Rn in the water column by <sup>226</sup>Ra decay ( $J_{\text{production}}$ );
- (3) surface inflow of Rn-rich water ( $J_{\text{inflow}}$ );
- (4) Rn loss across the air–water interface ( $J_{\text{atm}}$ );
- (5) Rn decay in the water column ( $J_{\text{decay}}$ );
- (6) surface outflow of Rn-rich water ( $J_{\text{outflow}}$ ).

The terms  $J_{\text{inflow}}$  and  $J_{\text{outflow}}$  have been taken into consideration only for Green Lake because of the presence of a stream (Acqua Amara) flowing in and another flowing out from the lake (see Fig. 2(a)). Neither surface water inflow nor outflow occurs in Black Lake.

The <sup>222</sup>Rn flux balance for Green lake can be written as

$$J_{\text{benthic}} + J_{\text{production}} + J_{\text{inflow}} - J_{\text{atm}} - J_{\text{decay}} - J_{\text{outflow}} = 0. \quad (1)$$

The approach was to assess all flux terms to estimate the total benthic flux required to support the Rn inventory by difference

$$J_{\text{benthic}} = J_{\text{atm}} + J_{\text{decay}} + J_{\text{outflow}} - J_{\text{production}} - J_{\text{inflow}} \quad (2)$$

Eq. (2) has been simplified for Black Lake, where no surface water inflow and outflow occur

$$J_{\text{benthic}} = J_{\text{atm}} + J_{\text{decay}} - J_{\text{production}} \quad (3)$$

If the total benthic flux exceeds the independently estimated diffusive flux from bottom sediments (see Section 4.5), the advective component can be calculated by difference

$$J_{\text{advective}} = J_{\text{benthic}} - J_{\text{diffusion}} \quad (4)$$

Estimates of the advective velocity of groundwater necessary to support the benthic fluxes can be obtained by establishing the tracer activity in the advecting fluids according to the following simple equation (Corbett et al., 2000):

$$\begin{aligned} \text{Groundwater velocity} \\ = J_{\text{advective}} / \text{Rn concentration in the advective fluids.} \end{aligned} \quad (5)$$

This velocity may then easily be converted into discharge units, if the area of the reservoir is taken into account

$$\begin{aligned} \text{Groundwater discharge} = \text{Groundwater velocity} \\ * \text{surface of the reservoir.} \end{aligned} \quad (6)$$

Chemical–physical parameters and  $^{222}\text{Rn}$  vertical profiles of Green and Black Lakes, as well as of spring water, have been used to identify the nature and the location of groundwater discharge into the lake and have shown the occurrence of water stratification.

#### 4.2. Fluxes to the atmosphere

The total flux of Rn to the atmosphere ( $J_{\text{atm}}$ ) can be calculated from the following equation taken from Corbett et al. (1997):

$$J_{\text{atm}} = k(C_w - \alpha C_a), \quad (7)$$

where  $C_w$  and  $C_a$  are the concentrations of Rn in the surface water and air, respectively ( $\text{Bq m}^{-3}$ );  $k$  is the gas transfer velocity ( $\text{m min}^{-1}$ ) and  $\alpha$ , is the Ostwald's solubility coefficient (dimensionless).

#### 4.3. Radon decay in the water column

A second output flux term to be considered in the  $^{222}\text{Rn}$  balance is the decay of  $^{222}\text{Rn}$  not supported by the decay of  $^{226}\text{Ra}$  in the water column ( $J_{\text{decay}}$ ). This can be calculated from

$$J_{\text{decay}} = \lambda C_{\text{Rn}}, \quad (8)$$

where  $\lambda$  is the decay constant of  $^{222}\text{Rn}$  (expressed in  $\text{min}^{-1}$ ) and  $C_{\text{Rn}}$  represents the whole lake  $^{222}\text{Rn}$  inventory, obtained by multiplying the inventory for each sampling station by a weighted area and then summing all the inventories.

#### 4.4. Surface outflow of radon-rich water

This output flux ( $J_{\text{outflow}}$ ) is due to the outflow of Rn-rich stream water from the lake. It has been considered only for the Green Lake balance. This can be calculated from:

$$J_{\text{outflow}} = Q * C / S, \quad (9)$$

where  $Q$  is the stream discharge ( $34 \text{ m}^3 \text{ min}^{-1}$  from Camponeschi and Nolasco, 1983),  $C$  is the Rn concentration in the stream water (chosen to be equal to the concentration of Rn in the surface water lake sampled in station 4, close to the lake outlet) and  $S$  is the surface of Green Lake ( $9660 \text{ m}^2$ ).

#### 4.5. Diffusion of $^{222}\text{Rn}$ from bottom sediments into overlying lake waters

The diffusion of  $^{222}\text{Rn}$  from bottom sediments provides some unsupported Rn to the overlying waters due to its relatively high solubility in the environment as a noble gas. In order to obtain the  $^{222}\text{Rn}$  diffusion flux ( $J_{\text{diffusion}}$ ), sediment equilibration experiments (Martens et al., 1980; Corbett et al., 1997, 2000) were performed. After at least a 30-day period, the equilibration activity of Rn supported by Ra in sediments was established and the  $^{222}\text{Rn}$  activity in water was measured. Assuming steady state conditions with negligible advective transport, the flux of Rn from the sediment was estimated:

$$J_{\text{diffusion}} = (\lambda D_s)^{1/2} (C_{\text{eq}} - C_0), \quad (10)$$

where  $\lambda$  is the decay constant of  $^{222}\text{Rn}$  ( $\text{min}^{-1}$ ),  $D_s$  is the effective wet bulk sediment diffusion coefficient in the sediments ( $\text{m}^2 \text{ min}^{-1}$ ),  $C_{\text{eq}}$  is the Rn concentration in pore fluids in equilibrium with Ra in the sediments ( $\text{Bq m}^{-3}$ ) and  $C_0$  is the Rn concentration in the overlying water at the sediment–water interface multiplied by the sediment porosity to obtain a wet sediment equivalent ( $\text{Bq m}^{-3}$ ).

#### 4.6. Production of $^{222}\text{Rn}$ in the water column

The production of  $^{222}\text{Rn}$  in the water column ( $J_{\text{production}}$ ) can be estimated from the following equation:

$$J_{\text{production}} = C_{\text{Ra}} * h * \lambda, \quad (11)$$

where  $\lambda$  is the decay constant of  $^{222}\text{Rn}$ ,  $C_{\text{Ra}}$  represents the average concentration of  $^{226}\text{Ra}$  in Green Lake and

Black Lake waters and  $h$  is the average depth of the lakes (8.5 m).

#### 4.7. Surface inflow of radon-rich water

This input flux ( $J_{\text{inflow}}$ ) is due to the flow of Rn-rich stream water into the lake. It has been considered only in Green Lake balance. This can be calculated from:

$$J_{\text{inflow}} = Q * C/S, \quad (12)$$

where  $Q$  is the stream discharge (Acqua Amara,  $3.24 \text{ m}^3 \text{ min}^{-1}$  from Camponeschi and Nolasco, 1983),  $C$  is the Rn concentration in the stream water (assumed to be equal to the Rn concentration of Sg13 and Sg14 springs) and  $S$  is the surface of Green Lake.

## 5. Results and discussion

### 5.1. Water chemistry

Results of physical and chemical analyses performed on lake and spring waters are reported in Tables 1a and 1b. Green Lake and Black Lake waters can be classified as Na–Cl type waters, because Na and Cl are the dominant ions. Sodium concentrations in Green Lake range from 405 to  $737 \text{ mg L}^{-1}$  and chlorides vary from 691 to  $1488 \text{ mg L}^{-1}$ , whereas Na and Cl contents in Black Lake are lower, ranging from 341 to  $413 \text{ mg L}^{-1}$  and between 518 and  $718 \text{ mg L}^{-1}$ , respectively. The chemistry of the lakes is unusual for a karst region and probably reflects the input of a deep groundwater component rich in Na and Cl ions mixing with the Ca– $\text{HCO}_3$  type waters from the Lepini karst ridge aquifer.

Conductivity values show the same difference in ion concentration between Green Lake ( $3.2\text{--}5.2 \text{ mS cm}^{-1}$ ) and Black Lake ( $2.7\text{--}3.0 \text{ mS cm}^{-1}$ ) demonstrating that Green Lake waters are slightly brackish and more saline than those of Black Lake. Conductivity distribution suggests that Green Lake was stratified in June 2002. A less dense and less saline water lens extending along the main axis of Green Lake (NE–SW oriented) overlaid colder and dense waters. Along Green Lake NE edge, where Sg13 and Sg14 springs emerge, fresher and less dense water seeps into the lake and moves upward. By comparing the chemical composition of the fresh lens recognised in Green Lake with that of Sg13 and Sg14 springs, it is evident that spring Sg14 belongs to the same type of Green Lake waters, whereas spring Sg13 can be classified as a Ca– $\text{HCO}_3$  type water. Spring Sg14 (locally known as “Acqua Zolfa”, because of the characteristic smell of  $\text{H}_2\text{S}$ ) can be related to the hydrothermal circuit existing in the buried karst bedrock of the Plain (Boni et al., 1980). Chemical data for lakes and springs plotted onto Schoeller diagrams (Figs. 3(a) and (b)) show that Green Lake, Black Lake and Sg14 waters have the same

chemical matrix displaying similar proportions among ions concentration, but higher contents of single ions in the lakes, probably because they receive the contribution of other springs, more mineralised than Sg14, namely “Acqua Amara” spring (spring n. 267 in Camponeschi and Nolasco, 1983, locally called “Amara” because of its bitter taste probably due to the high content of  $\text{MgSO}_4$ ) feeding the small stream flowing in NW Green Lake (see also Fig. 2(a)). This spring can be classified as Na–Cl type water, on the basis of the chemical analyses reported in Camponeschi and Nolasco (1983) and is probably related to the hydrothermal circuit existing in the buried karst bedrock of the Plain (Boni et al., 1980). Camponeschi and Nolasco (1983) reported that the spring was strongly mineralised (total solids dried at  $180 \text{ }^\circ\text{C}$  equal to  $2.8 \text{ g/L}$ ), with a temperature of  $22\text{--}23 \text{ }^\circ\text{C}$ .

The input of groundwater into Green Lake is also demonstrated by the low temperature (about  $11 \text{ }^\circ\text{C}$ ) recorded in sampling station 1 at  $-7 \text{ m}$  relative to the values ( $21\text{--}22 \text{ }^\circ\text{C}$ ) of surface waters in the month of June 2002 (see temperature profiles in Fig. 4(a)).

Temperature distribution in Black Lake showed that it was thermally stratified in July 2003, but no appreciable salinity stratification was detected. A 4-m thick water layer characterised by temperatures of  $27\text{--}29 \text{ }^\circ\text{C}$  overlay a colder water stratum with temperatures of  $9\text{--}10 \text{ }^\circ\text{C}$ . This colder fluid could represent an input of  $\text{HCO}_3$  type water infiltrating on top of Lepini Mounts karst ridge (above  $1400\text{--}1500 \text{ m asl}$ ) and emerging at the bottom of Black Lake. In order to keep that temperature, water circulation should be fast and could occur through a network of paleokarst conduits buried by the alluvial deposits of Pontina Plain, as hypothesised in the hydrogeological scheme of the Lepini Mounts ridge used by Petitta (1994) to numerically simulate the groundwater flow in this hydrogeological structure.

### 5.2. $\text{CaCO}_3/\text{CO}_2$ equilibria considerations

Green Lake waters are slightly acid; pH values range from 6.3 to 6.7, lower values having been detected in deepest samples from sampling station 1, where they approach those of spring Sg14. These pH values could be explained by deep  $\text{CO}_2$  gaseous sources ascending along the bordering fault systems and interacting with the Ca– $\text{HCO}_3$  type water from the karst aquifer, making them undersaturated. The hydration of deep  $\text{CO}_2$  produces  $\text{H}_2\text{CO}_3$  which, in turn, dissociates to provide abundant  $\text{H}^+$  and  $\text{HCO}_3^-$ . The addition of  $\text{H}^+$ , increases the  $\text{CaCO}_3$  solubility. This hypothesis is corroborated by the values of  $\text{pCO}_2$  up to  $0.40 \text{ atm}$  for Vescovo Lakes water reported in Salvati and Sasowsky (2002) and the high contents of  $\text{HCO}_3^-$  in lake water ( $621\text{--}1065 \text{ mg L}^{-1}$  in Green Lake and  $359\text{--}614 \text{ mg L}^{-1}$  in Black Lake) and spring water ( $376 \text{ mg L}^{-1}$  in Sg13,  $553 \text{ mg L}^{-1}$  in

Table 1a  
Hydrogeochemistry of groundwater and Green Lake

Sample	Depth (m)	T (°C)	pH	Conductivity (mS cm <sup>-1</sup> )	HCO <sub>3</sub> <sup>-</sup> (mg L <sup>-1</sup> )	Excess <sup>222</sup> Rn (Bq L <sup>-1</sup> )	F <sup>-</sup> (mg L <sup>-1</sup> )	SO <sub>4</sub> <sup>2-</sup> (mg L <sup>-1</sup> )	Cl <sup>-</sup> (mg L <sup>-1</sup> )	Ca <sup>2+</sup> (mg L <sup>-1</sup> )	Mg <sup>2+</sup> (mg L <sup>-1</sup> )	Na <sup>+</sup> (mg L <sup>-1</sup> )	K <sup>+</sup> (mg L <sup>-1</sup> )	SI
Spring Sg13	–	15.9	6.88	0.916	376	43.8	0.21	50	148	111	31	109	4	–0.14
Spring Sg14	–	16.6	6.45	2.29	553	43.8	0.25	118	515	180	49	323	10	–0.28
PSPP06 1A	–2	21.7	6.63	3.2	621	8.2	0.46	104	691	204	67	405	15	0.05
PSPP06 1B	–3	20.9	6.49	4.81	881	9.5	0.76	227	1328	311	106	718	34	0.15
PSPP06 1C	–6	20.5	6.29	3.85	920	15.8	0.78	272	1412	316	113	718	34	–0.03
PSPP06 1D	–7	11.4	6.3	5.11	913	3.7	0.78	173	1421	314	111	718	25	–0.16
PSPP06 2A	–2	21.6	6.48	3.13	730	6.1	0.41	139	697	213	63	415	15	–0.02
PSPP06 2B	–3	20.9	6.36	5.02	1025	4.0	0.67	188	1302	329	102	709	25	0.11
PSPP06 2C	–6	20.6	6.31	5.21	1057	0.7	0.7	180	1372	335	100	737	25	0.08
PSPP06 2D	–9	18.3	6.35	5.12	1041	0.0	0.68	189	1452	332	108	737	29	0.07
PSPP06 3A	–2	21.5	6.69	2.15	582	20.7	0.3	105	406	162	50	258	15	0.02
PSPP06 3B	–4	20.9	6.59	4.99	1030	5.0	0.63	193	1148	329	93	681	34	0.03
PSPP06 3C	–6	20.6	6.59	5.15	1059	2.8	0.63	146	1339	332	99	737	29	0.04
PSPP06 3D	–9	18.4	6.38	5.19	1041	0.2	0.63	185	1378	333	100	755	34	0.1
PSPP06 4A	–2	21.5	6.54	3.43	777	22.5	0.43	135	680	229	73	424	25	0.09
PSPP06 4B	–4	20.9	6.44	4.98	1014	12.8	0.6	178	1116	309	110	681	25	0.17
PSPP06 4C	–6	20.6	6.42	5.22	1065	10.0	0.64	151	1167	329	102	718	34	0.19
PSPP06 4D	–9	18.4	6.42	5.23	1065	2.0	0.41	159	1260	332	102	737	34	0.16
PSPP06 5A	–2	20.3	6.54	3.67	819	37.7	0.5	123	904	250	80	516	15	0.12
PSPP06 5B	–4	20.9	6.44	4.86	1017	26.2	0.63	180	1329	333	86	700	25	0.2
PSPP06 5C	–6	20.7	6.41	5.11	1062	15.7	0.7	153	1350	325	109	737	25	0.17
PSPP06 5D	–9	18.4	6.42	5.16	1030	2.8	0.75	–	1488	325	109	737	34	–

Samples labels PSPP06 is the reference number of Vescovo Lakes Group.

Numbers 1, 2, 3, 4 and 5 are the sampling stations at Green Lake and letters A, B, C and D stand for different water samples collected at increasing depth.

Table 1b  
Hydrochemical data of Black Lake

Sample	Depth (m)	T (°C)	pH	Conductivity (mS cm <sup>-1</sup> )	HCO <sub>3</sub> <sup>-</sup> (mg L <sup>-1</sup> )	Excess <sup>222</sup> Rn (Bq L <sup>-1</sup> )	F <sup>-</sup> (mg L <sup>-1</sup> )	SO <sub>4</sub> <sup>2-</sup> (mg L <sup>-1</sup> )	Cl <sup>-</sup> (mg L <sup>-1</sup> )	Ca <sup>2+</sup> (mg L <sup>-1</sup> )	Mg <sup>2+</sup> (mg L <sup>-1</sup> )	Na <sup>+</sup> (mg L <sup>-1</sup> )	K <sup>+</sup> (mg L <sup>-1</sup> )	SI
PSPP06 A1	-2	28.6	7.74	2.79	359	10.0	0.58	79	671	129	68	395	13	0.84
PSPP06 A2	-4	27.3	7.44	2.78	368	2.9	0.50	123	605	130	59	359	13	0.55
PSPP06 A3	-7	9.3	7.17	2.88	520	1.0	0.54	120	636	157	59	359	13	0.24
PSPP06 A4	-9	8.6	7.19	2.88	539	0.8	0.54	99	518	147	49	288	11	0.25
PSPP06 B1	-2	28.5	7.57	2.72	360	0.8	0.54	108	641	135	67	413	14	0.69
PSPP06 B2	-4	27.1	7.49	2.71	365	0.8	0.52	150	647	135	65	413	14	0.58
PSPP06 B3	-7	9.8	7.25	2.81	522	0.0	0.59	106	612	158	62	377	13	0.33
PSPP06 B4	-9	8.7	7.17	2.86	533	0.9	0.52	84	602	163	64	377	15	0.25
PSPP06 C1	-2	28.5	7.61	2.76	359	3.2	0.61	83	649	136	68	395	14	0.74
PSPP06 C2	-4	25	7.39	2.72	367	9.5	0.62	111	625	138	67	413	14	0.48
PSPP06 C3	-7	9	7.24	2.83	522	0.0	0.53	78	592	151	55	341	13	0.3
PSPP06 C4	-9	8.5	7.26	2.88	532	0.1	0.65	90	631	152	63	359	13	0.31
PSPP06 D1	-2	28.6	7.81	2.76	361	0.2	0.66	166	631	137	62	413	13	0.94
PSPP06 E1	-4	25.6	7.6	2.76	361	0.2	0.64	103	655	139	69	413	14	0.69
PSPP06 E2	-7	9.9	7.23	2.97	614	0.0	0.65	58	652	170	64	395	14	0.41
PSPP06 F1	-4	26.2	7.53	2.74	371	0.4	0.65	114	674	140	67	413	14	0.64
PSPP06 F2	-7	11.8	7.1	2.97	593	0.2	0.65	43	718	180	69	413	15	0.3
PSPP06 G1	-4	23.2	7.55	2.77	366	0.8	0.62	111	649	136	65	395	13	0.61
PSPP06 G2	-7	10	7.08	2.93	598	2.5	0.62	39	689	180	65	413	15	0.27

Letters A, B, C, D, E, F and G are the sampling stations at Black Lake and numbers 1, 2, 3 and 4 stand for different water samples collected at increasing depth.

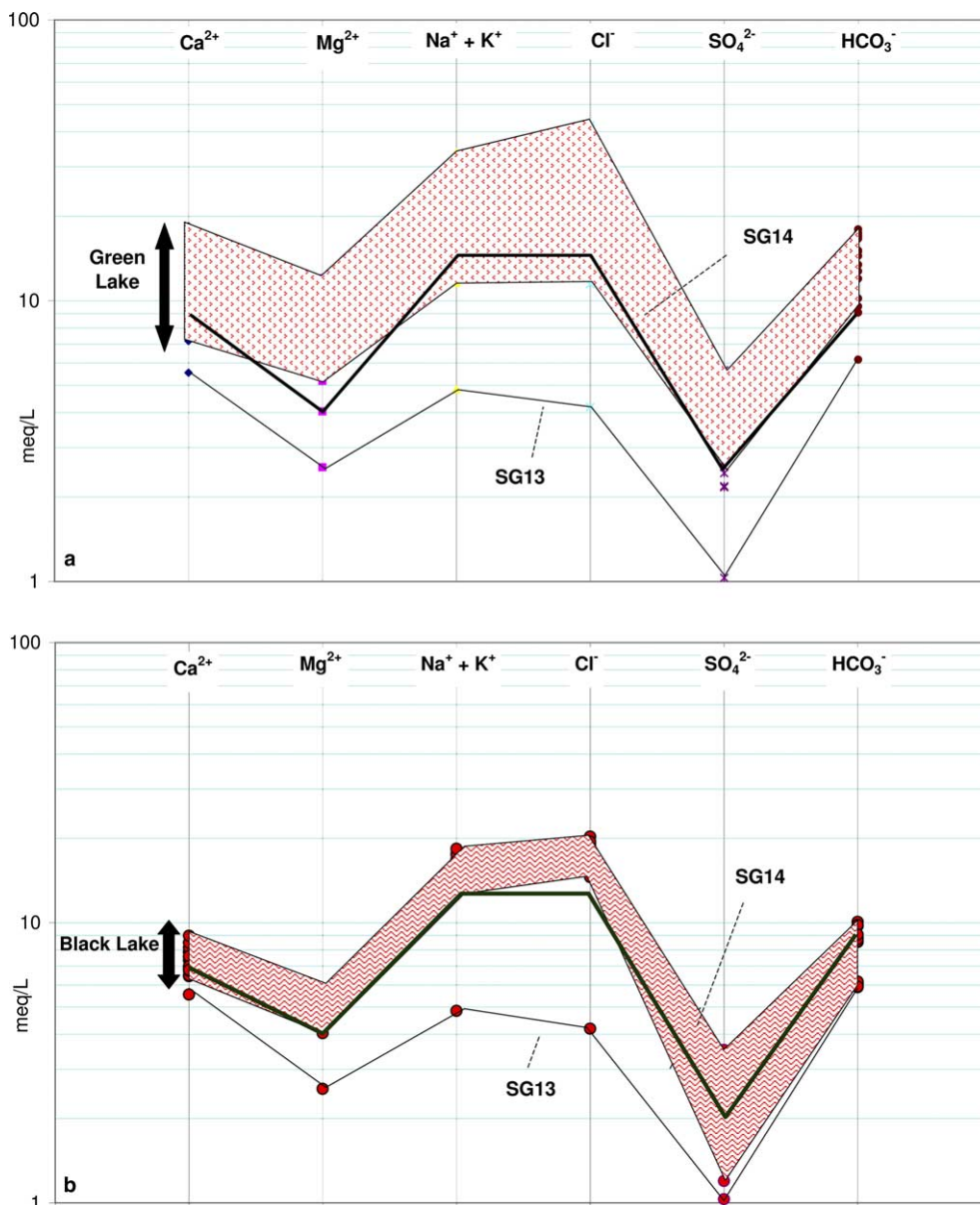


Fig. 3. Schoeller diagrams of Green Lake (a) and Black Lake (b) compared with Sg13 and Sg 14 springs.

Sg14 and  $1100 \text{ mg L}^{-1}$  in Acqua Amara, Camponeschi and Nolasco, 1983).

Also saturation indexes (SI) relative to calcite show the presence of unsaturated waters ( $\text{SI} = -0.16$ ) in the NE area of Green Lake. Negative SI have also been calculated for springs Sg13 and Sg14. Along the NE–SW oriented superficial lens extending along the main axis of Green Lake, waters are close to thermodynamic equilibrium, notwithstanding their low pH, probably because their  $\text{Ca}^{2+}$  and  $\text{HCO}_3^-$  concentrations, as well as their temperature, are higher than those of Sg13 and Sg14 springs, similarly characterised by low pH (6.88

and 6.45 respectively) These physical and chemical differences between spring water and lake water are probably due to the input of more mineralised spring water (Acqua Amara) into the lake. SI are positive (0.1–0.2) corresponding with sampling stations 4 and 5 (see Fig. 2(a)) where lake waters are now depositing travertine on the aquatic roots growing on the sinkhole's banks.

The pH values of Black Lake waters are always higher than 7, ranging between 7.1 and 7.7. The saturation index with respect to  $\text{CaCO}_3$  reaches values of 0.7–0.9 at the surface, decreasing down to 0.2–0.3 at depth. To

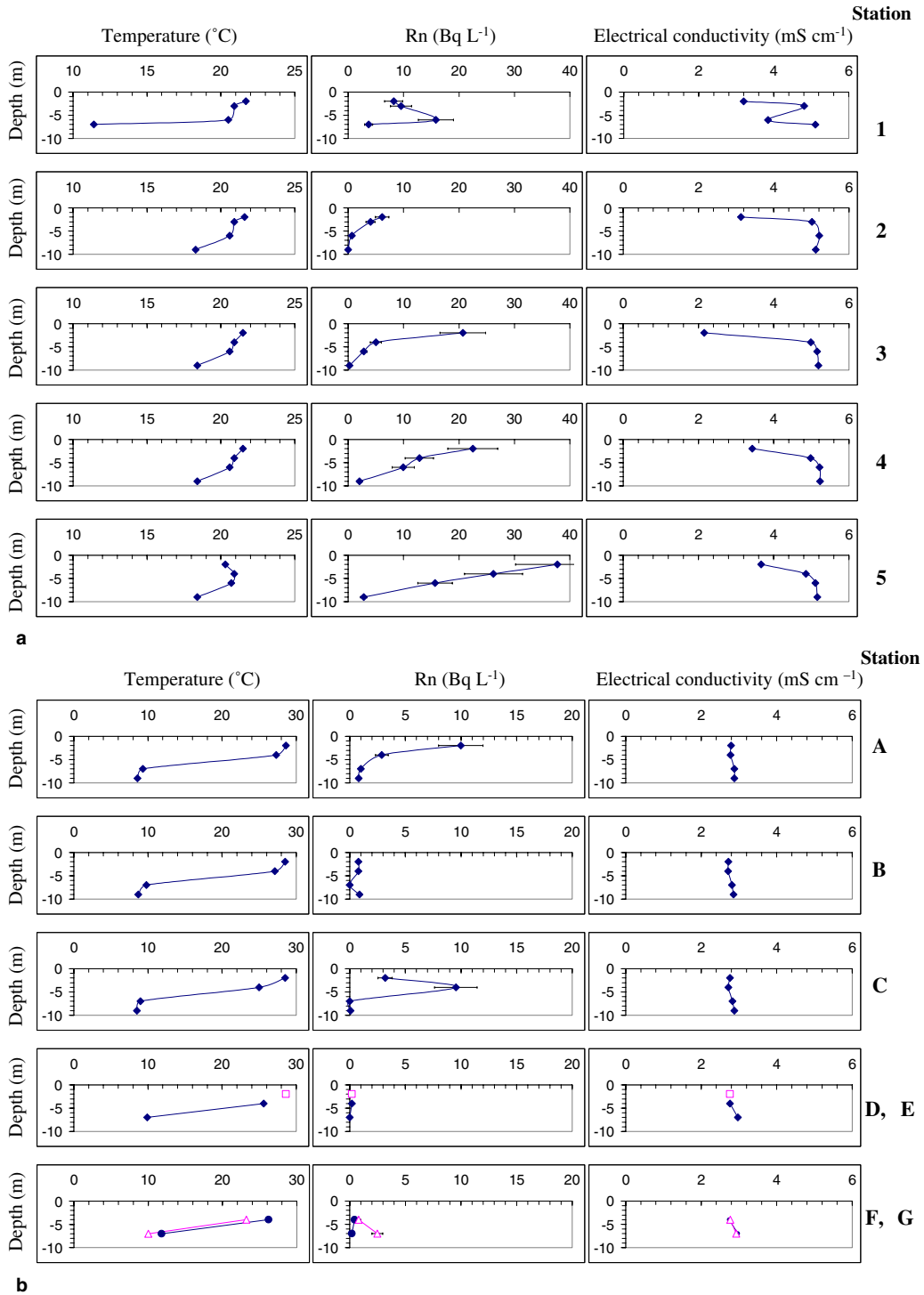


Fig. 4. Concentration of unsupported <sup>222</sup>Rn (Bq L<sup>-1</sup>), temperature (°C) and electrical conductivity (mS cm<sup>-1</sup>) versus depth (m) at station 1, 2, 3, 4 and 5 (Green Lake, a), A, B, C, D, E, F and G (Black Lake, b). The precision of unsupported <sup>222</sup>Rn calculations is mainly based on the precision of <sup>226</sup>Ra measurements and is around 20–25%.

corroborate the SI values, Black Lake waters are actively depositing travertine all around the sinkhole's border.

The high concentration of sulphates in lake water ( $104\text{--}272\text{ mg L}^{-1}$  in Green Lake and  $39\text{--}166\text{ mg L}^{-1}$  in Black Lake) and spring water ( $50\text{ mg L}^{-1}$  in Sg13,  $118\text{ mg L}^{-1}$  in Sg14 and  $116\text{ mg L}^{-1}$  in Acqua Amara, Camponeschi and Nolasco, 1983) can be explained by the oxidation of  $\text{H}_2\text{S}$  from deep-seated fluid circulation, interacting with  $\text{Ca-HCO}_3$  type water from the karst aquifer. Camponeschi and Nolasco (1983) reported a value of  $34\text{ mg L}^{-1}$  for  $\text{H}_2\text{S}$  in Acqua Amara water.  $\text{H}_2\text{S}$  may dissociate generating free  $\text{H}^+$  which may enhance carbonate dissolution.

Finally,  $\text{F}^-$  concentrations in Green Lake and Black Lake waters ( $0.3\text{--}0.8\text{ mg L}^{-1}$ ) exceed those of  $\text{Ca-HCO}_3$  type waters from Lepini karst ridge ( $0.045\text{ mg L}^{-1}$ , Boni et al., 1980) stressing the point that the latter mix with fluids enriched in  $\text{F}^-$ , probably from the hydrothermal circuit existing in the buried karst bedrock of the Plain (Camponeschi and Nolasco, 1983). The presence of  $\text{F}^-$  may be related to the dissolution of HF in water which also produces free  $\text{H}^+$  to further dissolve  $\text{CaCO}_3$ .

### 5.3. $^{222}\text{Rn}$ in groundwater, Green Lake and Black Lake

Depth profiles in the water columns of Green and Black Lake always showed an excess of  $^{222}\text{Rn}$  with respect to  $^{226}\text{Ra}$  ( $24.4 \pm 4.7\text{ Bq m}^{-3}$ ). In Green Lake

excess  $^{222}\text{Rn}$  depth profile recorded at sampling station 1 (Fig. 4(a)) indicates that groundwater enriched in  $^{222}\text{Rn}$  seeps into the lake at depth, moves upward, forming a lens of Rn-rich water extending towards the SW along the main axis of Green Lake along a density interface. The presence of a morphological threshold between sampling station 1 and the presumed location of groundwater discharge (probably corresponding with a depression in the lake bottom, see Fig. 5) influences the direction and the velocity of groundwater flow. Values of profiles at  $-6\text{ m}$  depth indicate that a groundwater flow (enriched in Rn and characterised by a lower EC) is directed upward where it immediately attains the temperature of the lake water (heat transfer by convection), whereas the flow of groundwater at  $-7\text{ m}$  depth is laminar because of the resistance encountered in contact with the lake bottom. This produces a reduction of groundwater velocity, the occurrence of a lens of lake water (depleted in  $^{222}\text{Rn}$  and characterised by higher electrical conductivity) underneath the groundwater and a fall in the efficiency of heat transfer which at the solid–water interface is transmitted mainly by conduction (see Figs. 4(a) and 5).

The presence of a superficial Rn-rich water lens along the main axis of Green Lake is clearly shown by the excess  $^{222}\text{Rn}$  depth profiles obtained at the other sampling stations (Fig. 4(a)), where surface water is greatly enriched in Rn with respect to bottom water. Superficial waters from sampling station 5 show the highest content

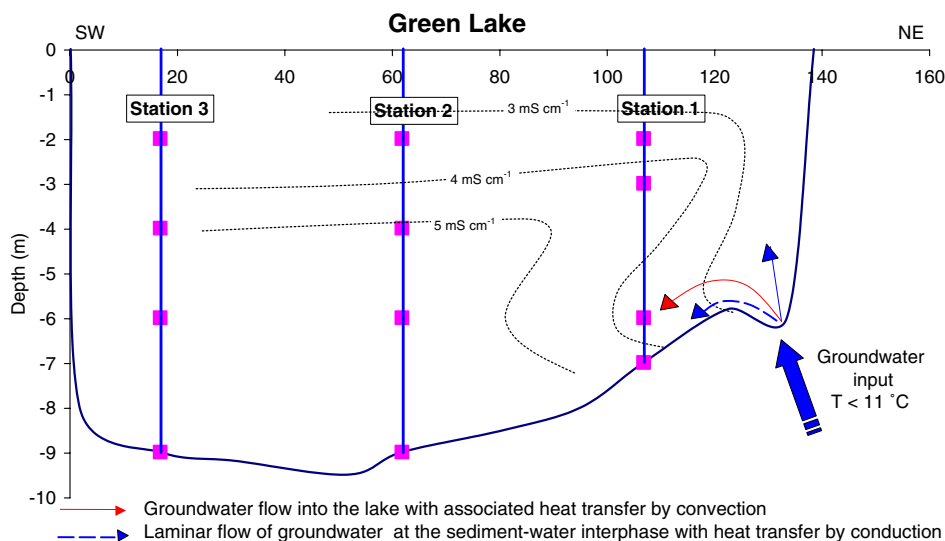


Fig. 5. Cross-sectional area along transect SW–NE, showing salinity stratification at Green Lake and groundwater flow into lake water, deducible from the electrical conductivity values recorded at sampling station 1, 2 and 3 (represented as solid vertical lines). Solid squares indicate the sampling depth, dashed lines show the indicative distribution of EC in lake water, thick arrow marks the input of groundwater corresponding with a depression in the lake bottom and other arrows represent groundwater flow into the lake at the sediment–water interface (dashed arrow) and further from it (solid arrow), with different heat transfer mechanism (see text for explanation).

of  $^{222}\text{Rn}$  ( $37.7 \text{ Bq L}^{-1}$ , see Table 1a). The  $^{222}\text{Rn}$  profile of sampling station 5 (Fig. 4(a)) can be explained by the presence of the Acqua Amara spring located a few tenths of metres to the NW of Green Lake and feeding a small stream, entering the lake in the area of sampling station 5. The inlet of this water (Fig. 2(a)), now hidden by aquatic plants but clearly mapped by Camponeschi and Nolasco (1983), is very close to the spring. This allows Rn from groundwater not to completely decay and being lost to the atmosphere before reaching the lake.

Excess Rn activities measured in Black Lake waters are lower than those of Green Lake, and close to zero in sampling station D, the area where North Black Lake and South Black Lake converge and the water depth is only 2 m. Black Lake excess  $^{222}\text{Rn}$  depth profile recorded at sampling station A and C (in North Black Lake) shows the highest  $^{222}\text{Rn}$  concentration at a depth of about 2 and 4 m respectively, whereas Rn profiles in South Black Lake record only a very small increase in Rn concentration in station G, at a depth of 7 m. The authors believe that excess  $^{222}\text{Rn}$  depth profiles in Black Lake, as well as in Green Lake, do not trace the exact location and depth of groundwater discharge because Rn transportation is determined primarily by diffusion patterns (influenced by the lake morphology) and the direction of the groundwater flow, but give a rough indication of the area where the discharge occurs. More precise information on the location of groundwater input can be derived from the lake bottom morphology and the water temperature. For these reasons it is hypothesised that groundwater seeps into Black Lake probably in the deepest part of North and South Black Lake, flows upward, and Rn diffuses in the direction of groundwater flow following the morphology of lake bottom.

Finally it is concluded, on the basis of the temperature depth profiles and the lake morphology, that Rn diffusion through the sediment/water interface is a point source diffusion. An advection–diffusion model (Corbett et al., 1997, 2000) has not been used to obtain the advective component because it is thought that the groundwater component in Green Lake and Black Lake is not diffuse source, but a point source which should not enhance the diffusion of Rn.

#### 5.4. Sediment results

Sediment equilibration experiments were used to estimate the diffusive fluxes of Rn from the lake bottoms (Table 2). The effective wet sediment diffusion coefficient ( $D_s$ ) used for these calculations was  $(7.5 \pm 1.9) \times 10^{-8} \text{ m}^2 \text{ min}^{-1}$ , after correcting for temperature and sediment tortuosity. This estimate is within experimental error of the literature values (Corbett et al., 1997). Sediment porosity was equal to  $0.88 \pm 0.06$  ( $n = 5$ ),  $C_{\text{eq}}$  was found to be  $1776 \pm 391 \text{ Bq m}^{-3}$  and  $C_0$  was  $523 \pm 120 \text{ Bq m}^{-3}$ . The total estimated diffusive flux from the lake bed was calculated from Eq. (10) and was equal to  $0.004 \pm 0.001 \text{ Bq m}^{-2} \text{ min}^{-1}$ .

#### 5.5. $^{222}\text{Rn}$ budget and estimates of groundwater contribution

By application of the model presented in Section 4, input and output fluxes of Rn were estimated for Green Lake in June 2002 and for Black Lake in July 2003 (Table 3). The precision of these flux calculations is mainly dependent on the precision of  $^{226}\text{Ra}$  and excess  $^{222}\text{Rn}$  measurements and ranges around 20–25%.

Output fluxes in Green Lake, represented by  $J_{\text{atm}}$ ,  $J_{\text{decay}}$  and  $J_{\text{outflow}}$ , were found to be  $10.5 \pm 2.1$ ,  $64.6 \pm 13.6$  and  $79.3 \pm 8.7 \text{ Bq m}^{-2} \text{ min}^{-1}$ , respectively. The value of parameters used to obtain the fluxes are reported in Table 2. To balance them, considering that  $J_{\text{production}}$  and  $J_{\text{inflow}}$  were found to be equal to  $0.0261 \pm 0.0005$  and  $14.7 \pm 1.5 \text{ Bq m}^{-2} \text{ min}^{-1}$ , respectively, a value of  $139.7 \pm 30.7 \text{ Bq m}^{-2} \text{ min}^{-1}$  was obtained for  $J_{\text{benthic}}$  from Eq. (2). Considering the value of  $0.004 \pm 0.001 \text{ Bq m}^{-2} \text{ min}^{-1}$  calculated for  $J_{\text{diffusion}}$  and using Eq. (4) a value of  $139.7 \pm 30.7 \text{ Bq m}^{-2} \text{ min}^{-1}$  was calculated for  $J_{\text{advective}}$ . This shows that advective transport of Rn associated with groundwater was the main Rn source to Green Lake in June 2002.

As far as Black Lake is concerned, two different balance calculations have been applied to North Black Lake and South Black Lake. Eq. (3) has been used in this case, because no lake inlet nor outlet is present. It must be outlined that the values of  $J_{\text{diffusion}}$  and

Table 2

Parameters used for flux calculations

Parameters used for flux calculations	Value
Gas transfer velocity ( $k$ , $\text{m min}^{-1}$ )	$(5.8 \pm 0.9) \times 10^{-4}$
Ostwald's solubility coefficient ( $\alpha$ , dimensionless)	0.25 at 20 °C
Porosity of lake sediments ( $\text{mL cm}^{-3}$ )	$0.88 \pm 0.06$
Effective Rn diffusion coefficient ( $\text{m}^2 \text{ min}^{-1}$ )	$(7.5 \pm 1.9) \times 10^{-8}$
$^{222}\text{Rn}$ equilibration activity ( $\text{Bq m}^{-3}$ porewater)	$1776 \pm 391$
Average $^{226}\text{Ra}$ in lake water ( $\text{Bq m}^{-3}$ )	$24.4 \pm 4.7$

The precision of  $^{226}\text{Ra}$  measurements and that of  $^{222}\text{Rn}$  equilibration activity is around 20–25%.

Table 3

Balance sheet drawing estimated input and output  $^{222}\text{Rn}$  fluxes for Green Lake and Black Lake, groundwater velocity and discharge

Fluxes ( $\text{Bq m}^{-2} \text{ min}^{-1}$ )	Green Lake	North Black Lake	South Black Lake
$J_{\text{atm}}$	$10.5 \pm 2.1$	$2.3 \pm 0.5$	$0.020 \pm 0.005$
$J_{\text{decay}}$	$64.6 \pm 13.6$	$10.1 \pm 2.1$	$1.5 \pm 0.4$
$J_{\text{outflow}}$	$79.3 \pm 8.7$	–	–
$J_{\text{production}}$	$0.0261 \pm 0.0005$	$0.0261 \pm 0.0005$	$0.0261 \pm 0.0005$
$J_{\text{inflow}}$	$14.7 \pm 1.5$	–	–
$J_{\text{diffusion}}$	$0.004 \pm 0.001$	$0.004 \pm 0.001$	$0.004 \pm 0.001$
$J_{\text{benthic}}$	$139.7 \pm 30.7$	$12.3 \pm 2.6$	$1.5 \pm 0.2$
$J_{\text{advective}}$	$139.7 \pm 30.7$	$12.3 \pm 2.6$	$1.5 \pm 0.2$
Groundwater velocity ( $\text{cm day}^{-1}$ )	$459 \pm 115$	$41 \pm 14$	$4.9 \pm 1.5$
Groundwater discharge ( $\text{L s}^{-1}$ )	$513 \pm 128$	$24 \pm 6$	$1.2 \pm 0.4$

The precision of Rn flux calculations, groundwater velocity and discharge are mainly dependent on the precision of  $^{226}\text{Ra}$  and excess  $^{222}\text{Rn}$  measurements and ranges around 20–25%.

$J_{\text{production}}$  used in these calculations are the same as used for Green Lake, because Black Lake sediments have been assumed to be similar to those of Green Lake and the average  $^{226}\text{Ra}$  activities ( $24.4 \pm 4.7 \text{ Bq m}^{-3}$ ) of the two lakes are the same. Output fluxes in North Black Lake, represented by  $J_{\text{atm}}$  and  $J_{\text{decay}}$ , were found to be  $2.3 \pm 0.5 \text{ Bq m}^{-2} \text{ min}^{-1}$  and  $10.1 \pm 2.1 \text{ Bq m}^{-2} \text{ min}^{-1}$ , respectively. The resulting  $J_{\text{advective}}$  was  $12.3 \pm 2.6 \text{ Bq m}^{-2} \text{ min}^{-1}$ , representing more than 99% of total Rn input.

$J_{\text{atm}}$  and  $J_{\text{decay}}$  of South Black Lake were  $0.020 \pm 0.005 \text{ Bq m}^{-2} \text{ min}^{-1}$  and  $1.5 \pm 0.4 \text{ Bq m}^{-2} \text{ min}^{-1}$ , respectively. The resulting  $J_{\text{advective}}$  was  $1.5 \pm 0.2 \text{ Bq m}^{-2} \text{ min}^{-1}$ , 99% of total Rn input in South Black Lake.

Estimates of the advective velocity of groundwater and groundwater discharge have been obtained for Green Lake and North and South Black Lake using Eqs. (5) and (6), respectively. The value of  $^{222}\text{Rn}$  concentration of springs Sg14 and Sg13 ( $43,808 \pm 8323 \text{ Bq m}^{-3}$ ) has been assigned to the advecting fluids in Eq. (5), because these springs are located on the NE edge of Green Lake where the input at depth of Rn-rich groundwater has been evidenced.

The resulting groundwater flow rate over the entire bed of Green Lake was equal to  $459 \pm 115 \text{ cm day}^{-1}$  and the total groundwater discharge was  $513 \pm 128 \text{ L s}^{-1}$ . The flow rate and the total discharge of groundwater into North Black Lake were  $41 \pm 14 \text{ cm day}^{-1}$  and  $24 \pm 6 \text{ L s}^{-1}$ , respectively. The groundwater flow rate over the bed of South Black Lake was  $4.9 \pm 1.5 \text{ cm day}^{-1}$  and the groundwater discharge was equal to  $1.2 \pm 0.4 \text{ L s}^{-1}$ .

The precision of these calculations is mainly dependent on that of  $^{226}\text{Ra}$  and excess  $^{222}\text{Rn}$  measurements and is about 25%.

### 5.6. Comparison with hydrological measurements

The groundwater contribution to Green Lake ( $513.4 \pm 128.3 \text{ L s}^{-1}$ ), North Black Lake ( $23.6 \pm 6.1$

$\text{L s}^{-1}$ ) and South Black Lake ( $1.2 \pm 0.4 \text{ L s}^{-1}$ ) calculated by application of a Rn tracing approach is in good agreement with more conventional hydrological measurements carried out in the area.

The sum of the total groundwater discharge into Green Lake, North Black Lake and South Black Lake ( $538.2 \pm 161.5 \text{ L s}^{-1}$ ) is in agreement with the total discharge measured in the months of June and July for the whole Vescovo Lakes Group outlet ( $716\text{--}888 \text{ L s}^{-1}$ , Ministero dei Lavori Pubblici and Servizio Idrografico, 1934). According to these values, the groundwater discharge estimated in this paper for Green Lake plus Black Lake represents 60–75% of the June–July discharge values measured for Vescovo Lakes outlet.

### 5.7. Groundwater circulation in the Lepini karst aquifer and sinkhole development

Hydrogeochemical and Rn analyses performed on Green Lake and Black Lake waters (Vescovo Lakes group) show that the two lakes are not simply “water filled” sinkholes, but springs.

The extent of groundwater discharge into the lakes has been calculated by application of a Rn budget, taking all output and input flux terms into consideration. The temperature depth profiles, along with the lake morphology, have suggested where the groundwater input occurs indicating that the groundwater component in Green Lake and Black Lake is not diffuse, but a point source probably located at the intersection of fault systems bordering the Lepini karst ridge with NE–SW oriented secondary tectonic elements. The water chemistry and Rn analyses have shown that groundwater, enriched in  $\text{Cl}^-$ ,  $\text{Na}^+$ ,  $\text{SO}_4^{2-}$ ,  $\text{F}^-$  and Rn, is acid (pH 6.3) and slightly undersaturated.

These fluids are responsible for the creation of voids at depth below the Pontina plain, either at the bedrock/sediment interface, or within the calcareous sediments within the overburden. Their undersaturation with respect to calcite is brought about by deep  $\text{CO}_2$  gaseous

sources ascending along the bordering fault systems and interacting with the Ca–HCO<sub>3</sub> type water from the karst aquifer. The hydration of deep CO<sub>2</sub> produces H<sub>2</sub>CO<sub>3</sub> which, in turn, dissociates to provide abundant H<sup>+</sup> and HCO<sub>3</sub><sup>-</sup>. The addition of H<sup>+</sup> related to this process enhances the CaCO<sub>3</sub> solubility.

Thermal data of the sublacustrine emergences (9–11 °C) indicate that a part of Lepini karst waters could flow along buried paleokarst conduits developed within the more permeable horizons of the limestone formations with a base level lower than the present one (Petitta, 1994). Similar paleokarst features have been

recognised in other downthrown limestone formations, covered by alluvial sediments and connected with sinkhole development (Kaufmann and Quinif, 1999). The suggested groundwater circulation conceptual model is shown in Fig. 6. Two different groundwater flowpaths are supposed to be at work in this frame; the shallower (flowpath A in Fig. 6), which is fast and fresher, should feed the basal springs located at the karst ridge/lowland interface. A second one (Flowpath B in Fig. 6), which is deeper, slower and more mineralised, should feed the thermomineral springs as well as the sinkhole lakes, interacting with deep seated fluxes (water and gases)

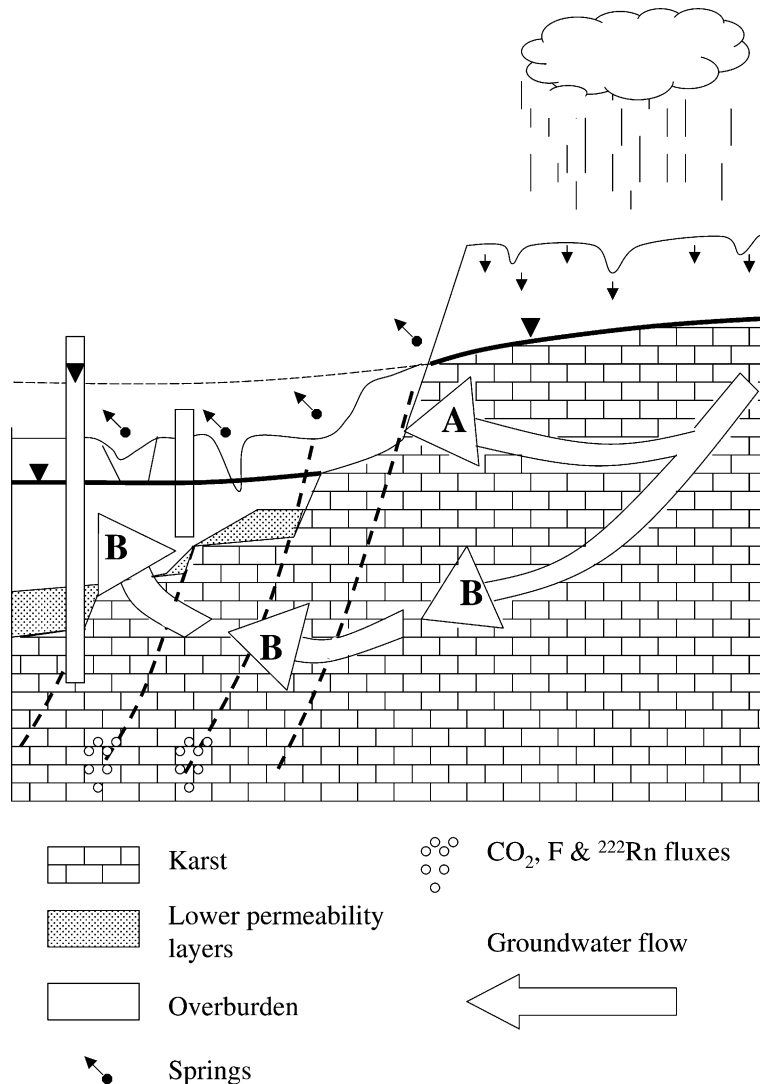


Fig. 6. Groundwater circulation in the Lepini Mounts karst aquifer. Two different flowpaths are hypothesised on the basis of the hydrogeochemical data. Path A corresponds to the present karst circuit and path B refers to the paleokarst network. Numbers from 1 to 3 along the flowpaths indicate a progressive saturation of the waters with respect to calcite. Numbers 4–5 represent a renewed undersaturation of waters due to the mixing with fluids, rich in CO<sub>2</sub>, F<sup>-</sup> and Rn, upwelling along the main faults bordering the karst ridge.

enriched in  $\text{Cl}^-$ ,  $\text{Na}^+$ ,  $\text{SO}_4^{2-}$ ,  $\text{F}^-$ ,  $\text{CO}_2$  and Rn upsurging along the main fault system bordering the karst ridge itself. A localised increase of permeability, associated with an increased temperature gradient along the deep faults bordering the karst ridge, enhance the upsurge of mineralised fluids.

## 6. Concluding remarks

Future collapses are to be expected in Pontina Plain (designated as a sinkhole prone area in the frame of the “Sinkhole Project” funded by Latium Region) at the intersection of fault systems bordering the Lepini karst ridge with NE–SW oriented secondary tectonic elements, which is characterised by the upsurge of deep-seated fluids rich in  $\text{CO}_2$  and  $\text{H}_2\text{S}$ . This is particularly true for the Vescovo Lakes Group, and Green Lake in particular, where a sudden collapse of the ground, immediately filled with water was observed and documented in 1991 (Piccozza, 2004). The collapse-driving fractures intersected the banks of an adjacent stream (Fiume Uffente, see Fig. 1) flowing over the ground level and caused the surrounding farmland to be submerged by flood water.

This suggests that it is difficult to predict when other collapse phenomena will occur, but it is important to monitor at least the areas where a collapse has already occurred in order to prevent further problems and hazards. The control of the area should start from monitoring the subsidence of the field, the opening of new fractures and also any bulging phenomena affecting the ground in the areas identified as sinkhole prone area in the frame of the “Latium Region Sinkhole Project”. The use of geophones to detect any small collapse at depth should help. A geochemical control of groundwater using monitoring wells is also recommended. Wells should be equipped with continuous probes measuring groundwater level, temperature, pH and conductivity to detect any change in groundwater level and chemistry connected to future collapses.

## Acknowledgements

We thank Dr. E. Hoehn for his helpful reviews. We are also grateful to Marco Conforti and Marco Garello for their assistance in the field and laboratory work. Marco Garello is also acknowledged for collection of underwater bottom sediments. Funding for this project was provided by Latium Region, Sinkhole Project.

## References

- Boni, C., Bono, P., Calderoni, G., Lombardi, S., Turi, B., 1980. Hydrogeological and geochemical analyses on the relationships between karst circulation and hydrothermal circuit in the Pontina Plain (Southern Latium). *Geologia Applicata e Idrogeologia* 15, 203–245.

- Bono, P., 1995. The sinkhole of Doganella (Pontina Plain, Central Italy). *Environ. Geol.* 26, 48–52.
- Cable, J.E., Burnett, W.C., Chanton, J.P., Weatherly, G.L., 1996. Estimating groundwater discharge into the northeastern Gulf of Mexico using radon-222. *Earth Planet. Sci. Lett.* 144, 591–604.
- Camponeschi, B., Nolasco, F., 1983. Le risorse naturali della Regione Lazio: Monti Lepini e Pianura Pontina. Regione Lazio, 8.
- Capelli, G., Petitta, M., Salvati, R., 2000. Strategic groundwater resources in Northern Latium volcanic complexes. Identification criteria and purposeful management. IAHS Publ. No. 272.
- Chanton, J.P., Burnett, W.C., William, C., Dulaiova, H., Corbett, D.R., Taniguchi, M., 2003. Seepage rate variability in Florida Bay driven by Atlantic tidal height. *Biogeochem.* 66, 187–202.
- Cook, P.J., Favreau, G., Dighton, J.C., Tickell, S., 2003. Determining natural groundwater influx to a tropical river using radon, chlorofluorocarbons and ionic environmental tracers. *J. Hydrol.* 277, 74–88.
- Corbett, D.R., Burnett, W.C., Cable, P.H., Clark, S.B., 1997. Radon tracing of groundwater input into Par Pond, Savannah River Site. *J. Hydrol.* 203, 209–227.
- Corbett, D.R., Dillon, K., Burnett, W.C., Chanton, J.P., 2000. Estimating the groundwater contribution into Florida Bay via natural tracers,  $^{222}\text{Rn}$  and  $\text{CH}_4$ . *Limnol. Oceanog.* 45, 1546–1557.
- Eaton, A.D., Clesceri, L.S., Greensberg, A.E. (Eds.), 1995. Standard Methods for the Examination of Water and Wastewater, nineteenth ed. American Public Health Association, Washington, DC.
- Ellins, K.K., Roman-Mas, A., Lee, R., 1990. Using  $^{222}\text{Rn}$  to examine groundwater/surface discharge interaction in the Rio Grande de Manati, Puerto Rico. *J. Hydrol.* 115, 319–341.
- Kaufmann, O., Quinif, Y., 1999. Cover-collapse sinkholes in the “Tournaisis” area, southern Belgium. *Eng. Geol.* 52, 15–22.
- Lambert, M.J., Burnett, C., 2003. Submarine groundwater discharge estimates at a Florida coastal site based on continuous radon measurements. *Biogeochem.* 66, 55–73.
- Lee, R.W., Hollyday, E.F., 1993. Use of radon measurements in Carters Creek, Maury County, Tennessee, to determine location and magnitude of ground-water seepage. In: Gundersen, L.C.S., Wanty, R.B. (Eds.), *Field Studies of Radon in Rocks, Soil and Water*. Smoley Publishing Company, pp. 237–242.
- Martens, C.S., Kippbut, G.W., Klump, J.V., 1980. Sediment–water chemical exchange in the coastal zone traced by in situ radon-222 flux measurements. *Science* 208, 285–288.
- Ministero Lavori Pubblici, Servizio Idrografico, 1934. Le sorgenti italiane. Elenco e descrizione. Agro Pontino e Bacino di Fondi. Istituto Poligrafico dello Stato, Roma, vol. 14, pp. 3–187.
- Moustafa, M.Z., Fontaine, T.D., Guardo, M., James, R.T., 1998. The response of a freshwater wetland to long-term

- 'low level' nutrient loads: nutrients and water budget. *Hydrobiol.* 364, 41–53.
- Michard, G., Sarazin, G., Jézéquel, D., Albéric, P., Ogier, S., 2001. Annual budget of chemical elements in a eutrophic lake, Aydat Lake (Puy-de-Dome), France. *Hydrobiol.* 459, 27–46.
- Petitta, M., 1994. Modelli matematici di simulazione dell'acquifero carsico dei Monti Lepini (Lazio Meridionale). Ph.D. Thesis, Univ. "La Sapienza", Rome, Italy.
- Piccozza, R., 2004. Evoluzione nel tempo dei Laghi del Vescovo: un esempio di sinkholes nella Pianura Pontina (Lazio sud-occidentale). In: Proc. Workshop "Stato dell'arte sullo studio dei fenomeni di sinkholes e ruolo delle amministrazioni statali e locali nel governo del territorio", APAT, Roma 2004.
- Salvati, R., Sasowsky, I.D., 2002. Development of collapse sinkholes in areas of groundwater discharge. *J. Hydrol.* 264, 1–11.
- Schwartz, M.C., 2003. Significant groundwater input to a coastal plain estuary: assessment form excess radon. *Estuar. Coast. Shelf Sci.* 56, 31–42.
- Smith, L., 2002. Using  $^{222}\text{Rn}$  activities to determine the extent of mixing between surface water and water of the Floridan aquifer. In: 2002 GSA Annual Meeting, Denver, Colorado, Abstracts with Programs, p. 497.
- Snow, D.D., Spalding, R.F., 1997. Short-term aquifer residence times estimated from  $^{222}\text{Rn}$  disequilibrium in artificially-recharged ground water. *J. Environ. Radioact.* 37, 307–325.
- Springer, C.E., 2004. Assessment of Groundwater Discharge to Lake Barco via Radon Tracing, Florida State University ETD Collection. Available from: <<http://etd.lib.fsu.edu/theses/available/etd-04052004-165926/>>, September 17th 2004.
- Wiegand, J., 2001. A guideline for the evaluation of the soil radon potential based on geogenic and anthropogenic parameters. *Environ. Geol.* 40, 949–963.